Worst Case Evaluation of Magnetic Field in the vicinity of Electric Power Substations

Gerhard Bräunlich #1, Reinhold Bräunlich *2

ETH Zürich, Switzerland
[1] g.braeunlich@gmail.com

* *FKH Fachkommission für Hochspannungsfragen*
Voltastr. 9, 8044 Zürich, Switzerland
[2] braeunlich@fkh.ch

***Abstract*—A simple procedure for the evaluation of magnetic field in the vicinity of substations is presented and discussed. The approach is based on the concept that all power installations can be decomposed into conductor loops and characterized by their magnetic dipole moment. A practical example for worst-case values of the magnetic stray flux is enclosed, where the effectiveness of the method is verified with practical measurements at a substation in well defined operation.**

I. Introduction

Electric power substations are often situated in industrial or residential areas where electrical installations are located close to working or living sites. According to national regulations the compliance with exposure limit values for the magnetic flux density have to be verified (in the Swiss ordinance relating to protection from non-ionising radiation [1] e.g. the precautionary limitation of emissions is $1\,\mu$T for sensitive used sites).

Electric power stations represent an accumulation of various electric devices, bus conductors and cable sections. A detailed computer model of the active installation requires the input of a large number of geometric data. As a consequence the sources of errors are numerous and careful model verification is necessary.

Since the magnetic field analysis of a power installation aims to check the compliance with emission limitations, a worst-case evaluation of the flux density at a defined location is adequate for this task. Frequently a determination of a maximum distance for the magnetic flux density to fall below a specified limit is of interest.

The present publication demonstrates the application of approximation formula for an evaluation of maximum flux density values in function of the distance. In all equations the rms values of a sinusoidal current I and correspondingly the rms magnitudes of the magnetic flux densities B [T] or [Vs/m^2] are being used if not stated otherwise:

$$B = \|B_{\mathrm{rms}}\| = \sqrt{\sum_{i=1}^{3}[\mathrm{Re}(B_i)]^2 + [\mathrm{Im}(B_i)]^2} \tag{1}$$

Arguments are the basic geometric parameters and the maximum values of current flowing in the phase conductors. It can be shown, that the simple approach does not lead to severe increase of uncertainty nor to a significant expansion of safety margins.

II. Magnetic dipoles of conductor loops for magnetic flux density evaluation

In the presented concept all installations are decomposed into conductor loops. The loops represent a magnetic dipole with the moment (2). For a complanate loop, the dipole moment reduces to the scalar expression (3).

$$\boldsymbol{m} = I \int_A \boldsymbol{\nu}\,\mathrm{d\,vol} \tag{2}$$

$$\boldsymbol{m} = AI\,\boldsymbol{\nu} \tag{3}$$

A: Surface bounded by the loop
$\boldsymbol{\nu}$: Unit normal vector on the surface A
I: Loop current

In the far field the magnitude of magnetic flux density B decreases with the inverse 3rd power of the distance r. In the direction of the dipole vector the magnetic flux density $B = B^{\perp}_{\mathrm{rms}}(r)$ is twice as high as in the direction parallel to the plane of the loop $B = B^{||}_{\mathrm{rms}}(r)$:

$$B^{\perp}_{\mathrm{rms}} = \frac{\mu_0 m}{2\pi}\frac{1}{r^3} \tag{4a}$$

$$B^{||}_{\mathrm{rms}} = \frac{\mu_0 m}{4\pi}\frac{1}{r^3} \tag{4b}$$

where $m = \|\boldsymbol{m}\|$. Obviously, for worst case considerations, relation (4a) can be applied in all directions. If a loop is not plane, the projection of its areas in three orthogonal space directions have to be considered separately and the total magnetic moment results from the vector sum of the three moments. (Fig. 1). An analytical proof is given in the appendix.

A. Three-phase lines and lower order magnetic moments

Line sections can be considered as long narrow loops. For two-phase lines of infinite length, the rms value of the flux density decays uniformly in all directions perpendicular to the line axis [2] (Fig. 2(a) and eq. (5)). For three-phase lines

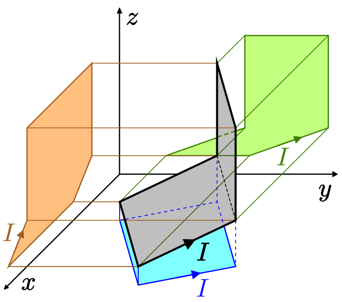

Figure 1. Projection of a non-complanate loop on three orthogonal planes

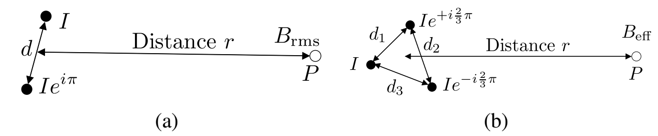

Figure 2. Definition of variables for the expression for the dipole magnetic flux density of (a) a two conductor line (eq. (5)) (b) a three-phase line (eq. (5) and (6))

with symmetrical currents the phase clearances (Fig. 2(b)) are composed according to eq. (6)

$$B_{\mathrm{rms}} \cong \frac{\mu d}{2\pi r^2} I_{\mathrm{rms}} \tag{5}$$

$$d = \sqrt{\frac{d_1^2 + d_2^2 + d_3^2}{2}} \tag{6}$$

For close distances from the observer to the three-phase conductors, the magnetic flux density will always be below the value given by eq. (7), if r is the shortest distances to a phase conductor.

$$B_{\mathrm{rms}} \leq \frac{\mu_0 I_{\mathrm{rms}}}{2\pi r} \frac{d}{\sqrt{r^2 + d^2}} \tag{7}$$

B. Three-phase line sections

For practical three-phase conductor sections such as bus bars, feeders and departures, the limited length of the sections has to be considered. The limitation in length results in a reduction of the magnetic flux density according to Fig. 3 and eq. (8).

$$B_{P\ \mathrm{rms}} \leq 2\sin(\alpha) B_{\mathrm{line}} = B_{\mathrm{line}} \frac{l}{\sqrt{r^2 + (l/2)^2}} \tag{8}$$

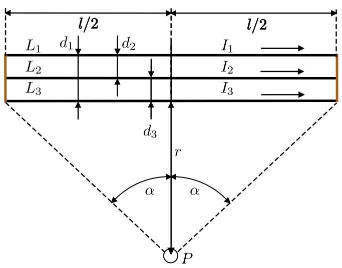

Figure 3. Explaining sketch for equation (8)

Finally, the magnetic flux density distribution of a three-phase section is limited by the general expression (9). For r, in a worst-case field evaluation again the shortest distance from the location of flux density evaluation to a conductor of the three-phase system must be chosen.

$$\boxed{B_{\mathrm{rms}} \leq \frac{\mu_0 I_{\mathrm{rms}}}{2\pi r} \frac{d}{\sqrt{r^2 + d^2}} \frac{l}{\sqrt{r^2 + (l/2)^2}}} \tag{9}$$

d: Combined phase distance according eq. (6)
l: Length of the considered three-phase section $[\mathrm{m}]$

Expression (9) consists of the following three terms:

1) The B_{rms} field of an infinitely long conductor
2) The sine of the angle at the point of observation subtended by the distance d
3) Twice the sine of the angle at the point of observation subtended by half of the length of the three-phase section $l/2$ (fig. 3)

III. Determination of the Distance from a Three-Phase Line Section to Keep to a Defined Magnetic Flux Density Limit

Unfortunately eq. (9) can not be solved explicitly for the distance r to evaluate the distance for a given value of B_{rms}. This disadvantage is overcome by an approximation of (9) by power functions in three sections (linear, square, cubic) (Fig. 4). The three approximating power functions (10) can be solved to r_c, being the necessary distance from the nearest conductor of the three-phase section to keep within the emission limit B_c.

$$r_{c1} = \frac{\mu_0 I}{2\pi B_c},\ r_{c2} = \left(\frac{\mu_0 I d}{2\pi B_c}\right)^{1/2},\ r_{c3} = \left(\frac{\mu_0 I d l}{2\pi B_c}\right)^{1/3} \tag{10}$$

The flux density remains within the limit B_c for r_c being the minimum value of r_{c1}, r_{c2} and r_{c3}. For $B_c = 1\,\mu\mathrm{T}$ the condition is expressed in eq. (11).

$$\begin{aligned} r_c[\mathrm{m}] = \min\{&0.2 \cdot I[\mathrm{A}], (0.2 \cdot I[\mathrm{A}] \cdot d[\mathrm{m}])^{1/2}, \\ &(0.2 \cdot I[\mathrm{A}] \cdot d[\mathrm{m}] \cdot l[\mathrm{m}])^{1/3}\} \end{aligned} \tag{11}$$

IV. Modelling of Substation Parts

A. Three-phase leads

The magnetic flux density of all three-phase lead or connection in an electric installation: bus-bar feeder etc. is modelled by one or several three-phase sections according to (9). It is important to point out, that every loop is necessarily closed at the interface to the neighbouring loop (Fig. 5(a) and Fig. 5(b)). Since the neighbour loop is closed as well, the closing currents cancel each other. A missing closing conductor would produce a second order decaying B-field magnitude, which would distort the far field dramatically.

In order to superimpose the magnetic flux densities of all different three-phase sections of an installation, the B_{rms} field of the sections may simply be summed up linearly. In the

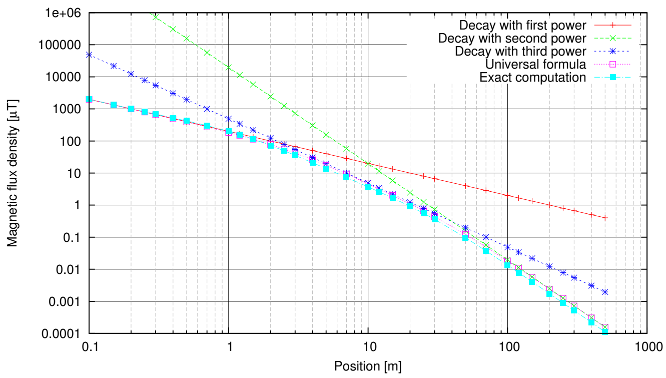

Figure 4. Decay of the magnetic flux density of a model conductor section according to Fig. 3 in the direction of point „P". The light blue curve shows the precise calculation. The violet trace marked by squares is the result of eq. (9). The traces of the functions (10) represent lines with different slope in the semi-logarithmic plot

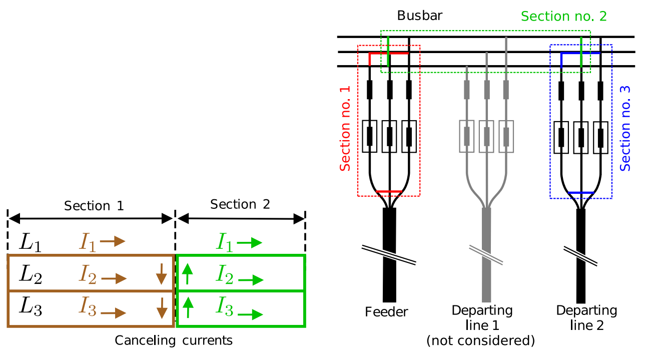

(a) (b)

Figure 5. (a) Division of a three-phase conductor system into two sections (b) Sketch of a small medium voltage switchgear. A proposal for a definition of three-phase sections (loops) is given representing the worst-case operating condition

sense of a worst-case evaluation the fact is disregarded, that the directions of the magnetic moments may not be aligned. The replacement of the proper vectorial summation by a scalar summation of the rms-values increases the calculated value and thus introduces a further safety margin into the evaluation. An important question is the determination of the nominal decisive operation state. For worst-case studies this is the most adverse operating condition. On HV level the current may be higher than the sum of the transformer input currents because of possible additional transit currents passing through the substation. In the medium voltage level, where transit currents normally do not exist, the maximum current is given by the nominal power of the transformers. In the medium voltage switchgear, the most adverse current distribution results if the current concentrates to the departing lines with largest distances to the transformer feeder. (Fig. 5(b)). Sections of the bus bar with differing currents are treated separately.

B. Transformers

According to theoretical consideration and practical measurements the magnetic flux density B of transformers and of

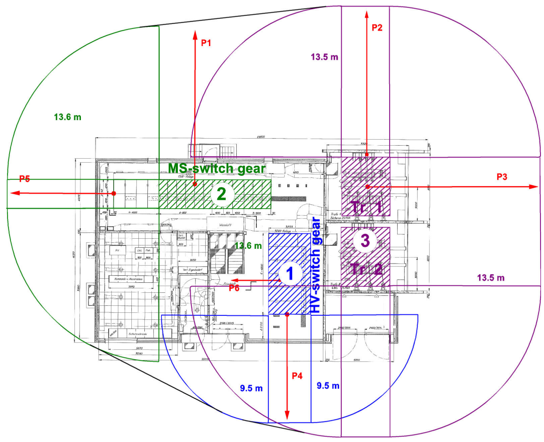

Figure 6. Result of a magnetic stray flux evaluation in a substation. The sum of maximum possible magnetic dipole moments for HV and MV switchgear and the transformers have been evaluated. The radius for the flux density to meet the emission limit of $1\,\mu\mathrm{T}$ is plotted around the active installations

other devices decrease with the third power of the distance. Practical experience suggests, that the magnetic dipole moment m and thus the stray flux density B is well related to the transformer nominal apparent power. Although proportionality to the square-root of the apparent power and to the relative short circuit voltage are proposed by some authors [3], our own measuring results in a wide power range demonstrated suitable worst-case values using the simple approach:

$$B_{\mathrm{rms}}(r) = k_{\mathrm{Tr}} \frac{P_N}{r^3} \tag{12}$$

P_N:	Nominal power of the transformer $[\mathrm{kVA}]$
r:	Distance from the centre of transformer $[\mathrm{m}]$
k_{Tr}:	Field coefficient $[\mathrm{ms/A}]$, $[\mathrm{Tm^3/VA}]$

An established value for k_{Tr} is $0.04\,\mathrm{Tm^3/kVA}$. With this expression the leads to the transformer-bushings are excluded and have to be calculated separately. The magnetic flux density of power devices can only be dominant, if they are placed at the outside edge of the installations. In distant positions of devices magnetic flux densities of lines and leads are dominant. With a $20\,\mathrm{MVA}$ transformer a reduction of the magnetic flux density to $1\,\mu\mathrm{T}$ is reached at a distance of $9\,\mathrm{m}$ from the transformer centre.

V. Example of the Magnetic Flux Density Evaluation of a Substation

An example for a theoretical evaluation of the worst case distance to reach a magnetic flux density below $1\,\mu\mathrm{T}$ for the installation is presented in Fig. 6 to 8. The investigated power substation was divided into the following main parts: 1) HV switchgear, 2) medium voltage switchgear, 3) transformers.

The parts of the power substation were considered as separate magnetic field sources. With the general approximation formula (9) the distances to meet the emission limits were determined in the most adverse operational situation at nominal current values. For the MV and HV switchgear 1), 2) and the transformer with connections 3), the effective

Figure 7. MV switchgear (left) and transformer (right), measuring profiles

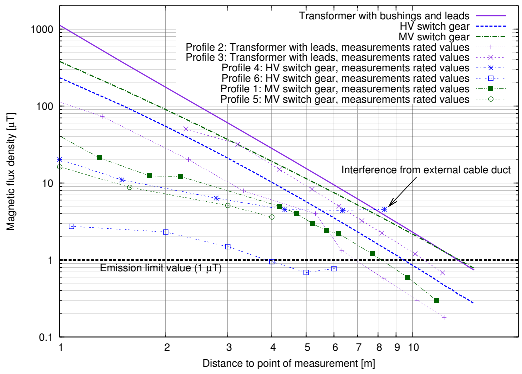

Figure 8. Theoretically evaluated and measured magnetic flux decay

geometric dimensions of the conductor arrangement have been used. For the reporting contour lines with the determined distances, measured from the current carrying conductors were plotted (Fig. 6) and compared with the measured results (Fig. 8).

VI. Conclusion

A quick method for the worst-case evaluation of magnetic field of power substations has been introduced and the application for practical cases is demonstrated. The procedure bases on the concept, that all installations can be decomposed into conductor loops which can be characterized by their magnetic dipole moments rendering simple expressions for the magnetic flux density values B_{rms}. For worst-case evaluation a scalar summation is proposed to obtain maximum values for the magnetic flux density in the vicinity of the installation or the distances to keep to emission limits. HV and MV switchgear and the transformer installation have been evaluated separately and the results have been superimposed. The theoretical results have been verified by practical measurements at operating substations.

Acknowledgment

The Authors thank Elektra Baselland EBL, Liestal, Switzerland for support during elaboration of the presented worst-case evaluation method. Thanks appertains to Dr. Vahe der Houhanessian, FKH for the guidance of the field measurements.

References

[1] Swiss Federal Council, "Ordinance relating to protection from non-ionising radiation (ONIR)," *SR 814.710*, Feb. 1 2000.

[2] W. T. Kaune and L. E. Zafanella, "Analysis of magnetic fields produced far from electric power lines," *IEEE Transactions on Power Delivery*, vol. 7, no. 4, pp. 2082–2091, Oct. 1992.

[3] F. Alber, "Verteiltransformatoren und EMV," *etz*, vol. 115, no. 20, pp. 1174–1177, 1994.

Appendix

Proof: The magnetic dipole moment of a non-complanate loop is the vectorial sum of the moments of the orthogonal projections of this loop

The magnetic moment of a closed loop is given by

$$\boldsymbol{m} = \frac{I}{2}\int_{\gamma=\partial M} \boldsymbol{\gamma} \times \mathrm{d}\boldsymbol{\gamma} = I \int_M \boldsymbol{\nu}\, \mathrm{d}\,\mathrm{vol}\,, \tag{13}$$

where M is a two-dimensional compact manifold $M \subset \mathbb{R}^3$ with boundary ∂M, corresponding atlas and partition of unity $\{(U^{(j)}, \boldsymbol{\phi}^{(j)}, \rho^{(j)})\}$, $j = 1, \ldots, N$ and $\boldsymbol{\nu}$ is the unit normal vector on M. M is locally the graph of some functions $\varphi^{(j)} : V^{(j)} \to \mathbb{R}$, i.e. the $\boldsymbol{\phi}^{(j)} : U^{(j)} \to V^{(j)} \subset \mathbb{R}^2$ are projections onto either the x-y-plane (type (z)), the x-z-plane (type (y)) or the y-z-plane (type (x)).

In a chart $(U^{(z)}, \boldsymbol{\phi}^{(z)})$ of type (z), we have

$$(\boldsymbol{\phi}^{(j)})^{-1}(x, y) = \begin{pmatrix} x \\ y \\ \varphi^{(j)}(x, y) \end{pmatrix}$$

and

$$\begin{aligned} \mathrm{d}\boldsymbol{\sigma}^{(z)} &= \frac{\partial(\boldsymbol{\phi}^{(z)})^{-1}}{\partial x} \times \frac{\partial(\boldsymbol{\phi}^{(z)})^{-1}}{\partial y} \mathrm{d}x\,\mathrm{d}y \\ &= \begin{pmatrix} -\frac{\partial\varphi^{(z)}}{\partial x} \\ -\frac{\partial\varphi^{(z)}}{\partial y} \\ 1 \end{pmatrix} \mathrm{d}x\,\mathrm{d}y \end{aligned} \tag{14}$$

up to a sign for the orientation. The z-component of

$$\boldsymbol{\sigma}^{(z)} = \int_{U^{(z)}} \boldsymbol{\nu}\mathrm{d}\,\mathrm{vol} = \int_{V^{(z)}} \mathrm{d}\boldsymbol{\sigma}^{(z)}$$

thus is the area of $V^{(z)}$.

Consider now the contribution to the z-component of $\boldsymbol{\sigma} := \boldsymbol{m}/I$ from a overlapping part $U^{(x)} \cap U^{(z)}$ of a chart $(U^{(x)}, \boldsymbol{\phi}^{(x)})$ of type (x), overlapping with $U^{(z)}$. It is again the area of the projection of the overlapping onto the x-y-plane, because the integrals of $\boldsymbol{\nu}$ over $U^{(x)} \cap U^{(z)}$ in both charts have to agree.

Integrating over whole M using the partition of unity yields that the components of $\boldsymbol{\sigma}$ are the areas of the projections of M onto the corresponding coordinate planes. Charts with opposite orientations cancel each other.

As a summary of the above, the following relation can be given

$$\mathrm{area}[\pi_{\boldsymbol{e}}(M)] = \boldsymbol{\sigma} \cdot \boldsymbol{e}, \tag{15}$$

where $\pi_{\boldsymbol{e}}(M)$ is the projection of M onto the plane perpendicular to the unit vector $\boldsymbol{e}$ through the origin. An immediate consequence is the fact, that the area of the projection of M is maximal if the projection is along $\boldsymbol{\sigma}$.